JOURNAL OF MATERIALS SCIENCE **35** (2000) 3733–3739

High-temperature stability of low-oxygen silicon carbide fiber heat-treated under different atmosphere

T. SHIMOO, K. OKAMURA
Department of Metallurgy and Materials Science, College of Engineering, Osaka Prefecture University, 1-1, Gakuen-cho, Sakai, Osaka 599-8531, Japan
E-mail: shimoo@mtl.osakafu-u.ac.jp

M. ITO
Graduate Student, Osaka Prefecture University, 1-1, Gakuen-cho, Sakai, Osaka 599-8531, Japan

M. TAKEDA
Nippon Carbon Co. Ltd., Shin-urashima-cho, Kanagawa-ku, Yokohama, Kanagawa, 221-0031, Japan

The effects of heat-treating atmosphere on the thermal stability of low-oxygen silicon carbide fiber were investigated. Heat-treatment of EB-cured PCS fiber were conducted at 1573 K in argon, nitrogen or vacuum of 10^{-6} atm. Subsequently the fibers were exposed to 1873 K in argon. The strength of fibers were strongly influenced by the heat-treating atmosphere. When heat-treated in nitrogen, the fibers absorbed nitrogen. High-temperature exposure caused severe degradation of strength owing to the decomposition of silicon oxycarbonitride phase. When heat-treated in vacuum, the fiber surface was smooth and pore-free, minimizing the degradation of strength at high temperature. *© 2000 Kluwer Academic Publishers*

1. Introduction

Ceramic material is employed for high-temperature structural applications because of its high melting point, high temperature strength, stiffness and oxidation resistance. However, the use of ceramic material must be restricted because of its low fracture toughness. The method for the maintenance of mechanical reliability at elevated temperature is the strengthening of ceramic material with continuous ceramic fiber. The polycarbosilane (PCS)-derived silicon carbide fiber is of great importance as a reinforcing material to a ceramic-matrix composites. Now, such fibers are commercially available as Nicalon and Hi-Nicalon (Nippon Carbon Co., Tokyo, Japan). Since Nicalon fiber is prepared by the oxidation-curing method, it contains oxygen of 15 mass% in concentration. Oxygen exists in the fiber as amorphous silicon oxycarbide (SiC_XO_Y) phase, mixed with SiC nanocrystallite and free carbon [1]. At elevated temperature, SiC_XO_Y phase has a tendency to crystallize into β-SiC, being accompanied by the generation of SiO and CO gases. As a consequence of the coarsening of β-SiC crystal and the damage to fiber structure, Nicalon fiber deteriorates significantly above 1573 K [2–9]. The elimination of oxygen from silicon carbide fiber could be achieved by introducing the electron-beam irradiation (EB) curing method. The strength of Hi-Nicalon fiber prepared in this method was retained in considerable level even at 1873 K because of low-oxygen content [10, 11].

The establishment of the most appropriate heat-treatment for EB-cured PCS fiber is required in order to improve further the thermal stability of Hi-Nicalon fiber. Previously, the EB-cured PCS fiber has been heat-treated in argon by changing the heat-treatment conditions such as heating rate, temperature and duration [12–14]. In present work, the effect of heat-treatment atmosphere on the high-temperature stability of low-oxygen silicon carbide fiber was investigated. EB-cured fiber was heat-treated at 1573 K under each atmosphere of argon, nitrogen and vacuum., and subsequently it was exposed to 1873 K in argon. The chemical, microstructural and mechanical examinations were carried out for both the as-heat treated fibers and the fibers exposed to 1873 K.

2. Experimental procedure

The specimen employed in this study is the electron beam-cured polycarbosilane (EB-cured PCS) fiber supplied by Nippon Carbon Co. (Tokyo, Japan). It has a molar composition of $SiC_{1.83}O_{0.035}H_{3.78}$ and an average diameter of 23.5 μm.

The heat-treatment of EB-cured PCS fibers were performed in an SiC resistance–heated, horizontal

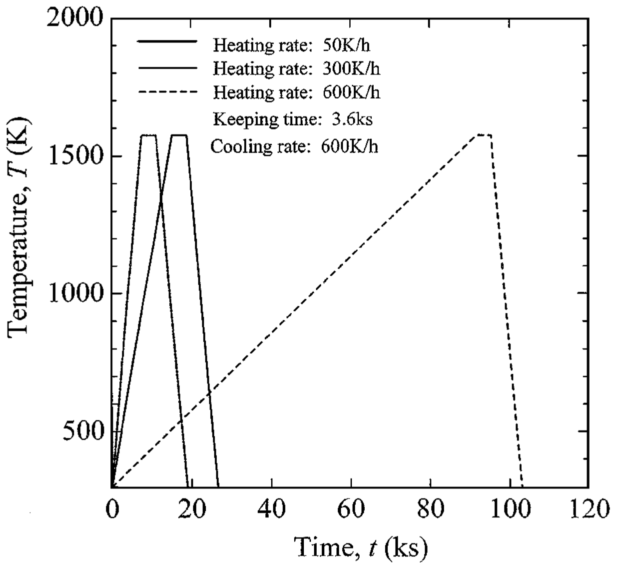

Figure 1 Heat-treatment cycles of EB-cured PCS fiber.

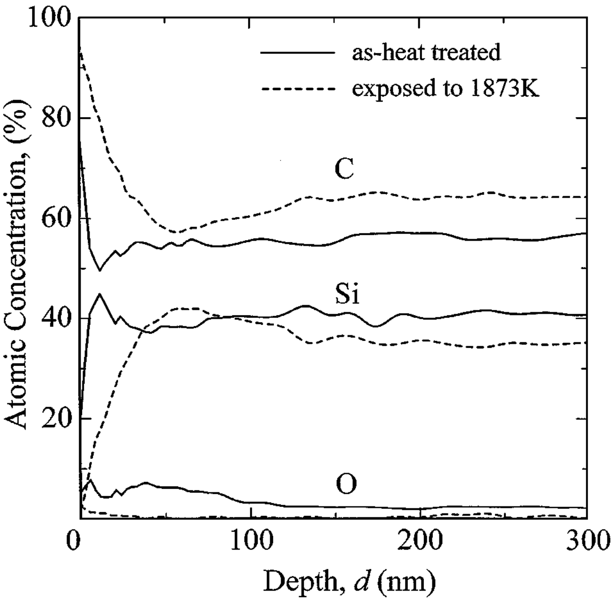

Figure 2 AES depth profile heat-treated at 50 K/h in argon.

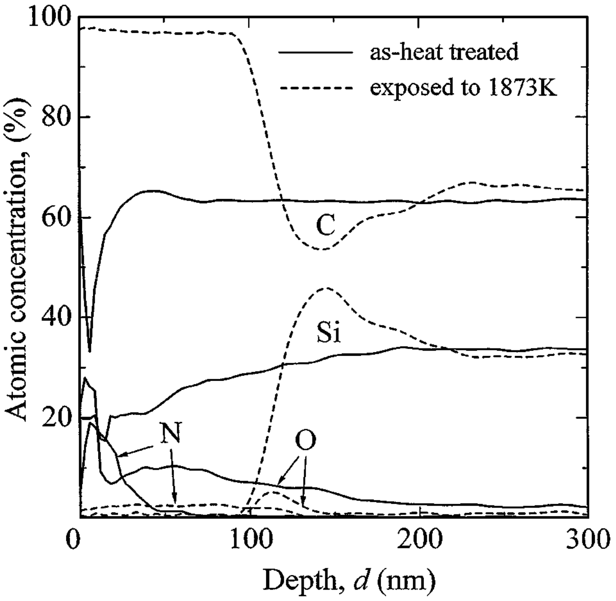

Figure 3 AES depth profile of fiber heat-treated at 50 K/h in nitrogen.

alumina-tube furnace. 4 g of fibers, 15 cm in length were placed in an alumina boat and were heated continuously from room temperature to 1573 K in argon, nitrogen or vacuum of 10^{-6} atm. The heating rate was 50, 300 or 600 K/h and the holding time at 1573 K was 3.6 ks. The cycles of heat-treatment are shown in Fig. 1. In order to evaluate the thermal stability of the heat-treated fibers (low-oxygen silicon carbide fiber), they were subsequently subjected to a high-temperature exposure test. The fibers placed in a graphite crucible were put into the carbon-resistance furnace (Tanmann furnace) which was regulated to 1873 K, and were kept for 3.6 ks in argon.

Auger electron spectroscopy (AES) characterization was carried out for the surface composition of fibers. The existing phases in the fibers were identified by X-ray diffraction and the morphologies of fibers were examined using the field emission scanning electron microscope (Hitachi Limited., Type S5400, Tokyo, Japan). The specific resistivity of fibers was determined at room temperature by applying direct current. Both ends of a fiber were attached with electroconductive resin to copper electrode plates which were 0.8 mm apart in distance. The average of ten measurements was taken as the specific resistivity at each heat-treatment condition. The room-temperature strength of a fiber of 10 mm gauge length was measured with a tensile tester (Orientec Co., TENSILON UTM-II-20, Tokyo, Japan) using a load cell of 100 g and a constant crosshead speed of 2 mm/min. The mean value of twenty tensile testing was taken for each fiber.

3. Results

3.1. AES depth profile

Fig. 2 shows the AES depth profile of the fiber heat-treated in argon. While the oxygen, with which PCS fiber was presumably contaminated during EB-curing, was retained after the heat-treatment, a very thin carbon-enriched layer of about 4 nm was formed on the surface. The exposure of 3.6 ks to 1873 K resulted in the nearly perfect removal of oxygen and the development of carbon-enriched layer. In addition, there was the increase of C/Si mole ratio from 1.4 to 1.8 in fiber core, suggesting the volatilization of silicon.

The AES depth profile of the fiber heat-treated in nitrogen is shown in Fig. 3. In comparison to the fiber heat-treated in argon, oxygen was highly concentrated at the fiber surface. It may be noted that nitrogen was contained up to about 80 nm depth in the as-heat treated state. This is because the absorption of nitrogen from the atmosphere took place during heat treatment. In particular, the fiber surface was enriched in both oxygen and nitrogen up to about 10 nm in thickness. Amorphous silicon oxycarbonitride ($SiC_XO_YN_Z$) phase is thought to be formed in this region [15]. When exposed to 1873 K, there was marked change in the surface composition. On the other hand, there was only a slight change in the core composition. Oxygen and nitrogen were removed nearly completely throughout the fiber, and the carbon-enriched layer (that is, silicon-depleted layer) was formed up to a depth of about 100 nm. The decomposition of $SiC_XO_YN_Z$ phase appears to be permitted to evaporate silicon in addition to oxygen and nitrogen.

Fig. 4 shows the AES depth profile of the fiber heat-treated in vacuum. Even in the as-heat treated state, oxygen was completely removed and a carbon-enriched layer of 40 nm depth was formed. Therefore, the exposure to 1873 K caused little change in the AES depth profile. AES depth profiles were quite similar to that of the fiber which was heat-treated in argon and was subsequently to 1873 K (Fig. 2). Therefore, both oxygen and silicon are considered to evaporate already during vacuum heat-treatment.

3.2. Specific resistivity

The specific resistivity of the fibers heat-treated under different conditions is shown in Fig. 5. For the fibers heat-treated in argon, the resistivity was practically unaffected by heating rate, and the exposure to 1873 K allowed to decrease the resistivity by a factor of 3. On the other hand, the resistivity of the fibers heat-treated in nitrogen had a tendency to decrease with an increase in heating rate. In addition, the high-temperature exposure caused large decrease in the resistivity. This can be probably attributable to the formation of $SiC_XO_YN_Z$ phase and the resulting change in surface composition (see Fig. 3). The vacuum heat-treatment gave the lowest levels of resistivity and was comparable with that of the fibers which were exposed to 1873 K after the heat-treatment in nitrogen and argon. The high-temperature exposure of the vacuum heat-treated fiber caused only a slight change in resistivity from 2×10^{-3} to 1×10^{-3} Ω m. Therefore, for the vacuum heat-treated fiber, the exposure to 1873 K is thought to cause little the microstructural change.

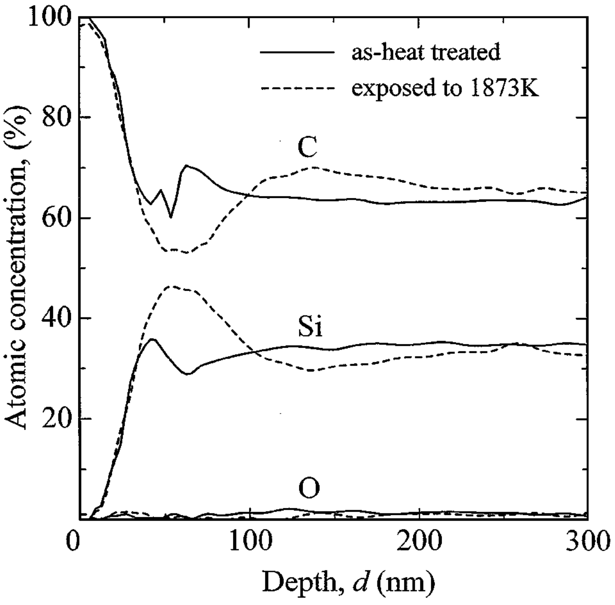

Figure 4 AES depth profile of fiber heat-treated at 50 K/h in vacuum.

3.3. Crystallite size of β-SiC

The silicon carbide fibers, in the heat-treated state and after the high-temperature exposure, were analyzed by X-ray diffraction. The apparent crystallite size of β-SiC, D_{SiC}, which was calculated from the half-value width of the (111) peak of β-SiC using the Scherrer formula, is shown in Fig. 6. In all the heat-treatment conditions, the crystallite size had a tendency to increase with increasing the heating rate. The value D_{SiC}, which was in the range of 3.5 to 5 nm. in the as-heat treated state, increased by a factor of 2 – 3 after 3.6 ks of exposure to 1873 K. In particular, the high-temperature exposure caused marked increase in the β-SiC crystal size of the vacuum heat-treated fiber.

3.4. Morphology

The morphologies of the fibers, which were exposed to 1873 K in argon, are shown in Fig. 7. The fibers

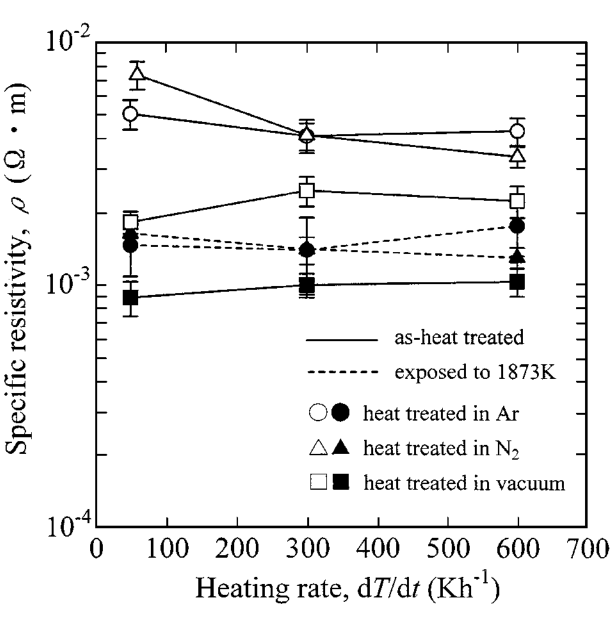

Figure 5 Specific resistivity of fibers heat-treated under different atmospheres.

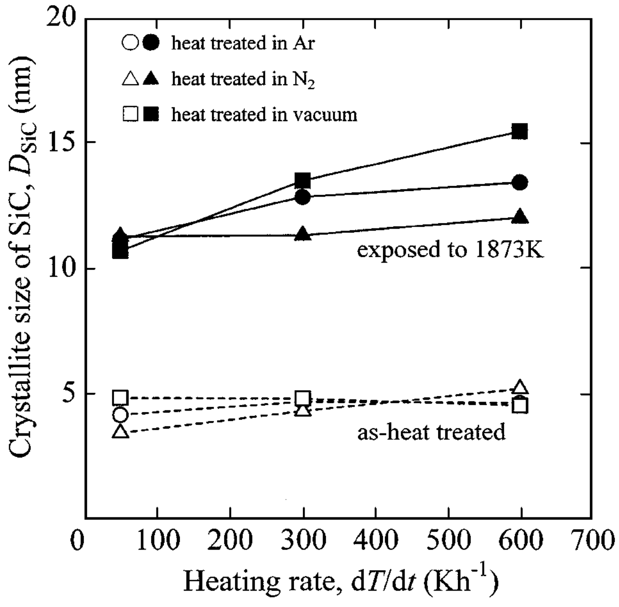

Figure 6 Apparent crystallite size of SiC for fibers heat-treated under different atmospheres.

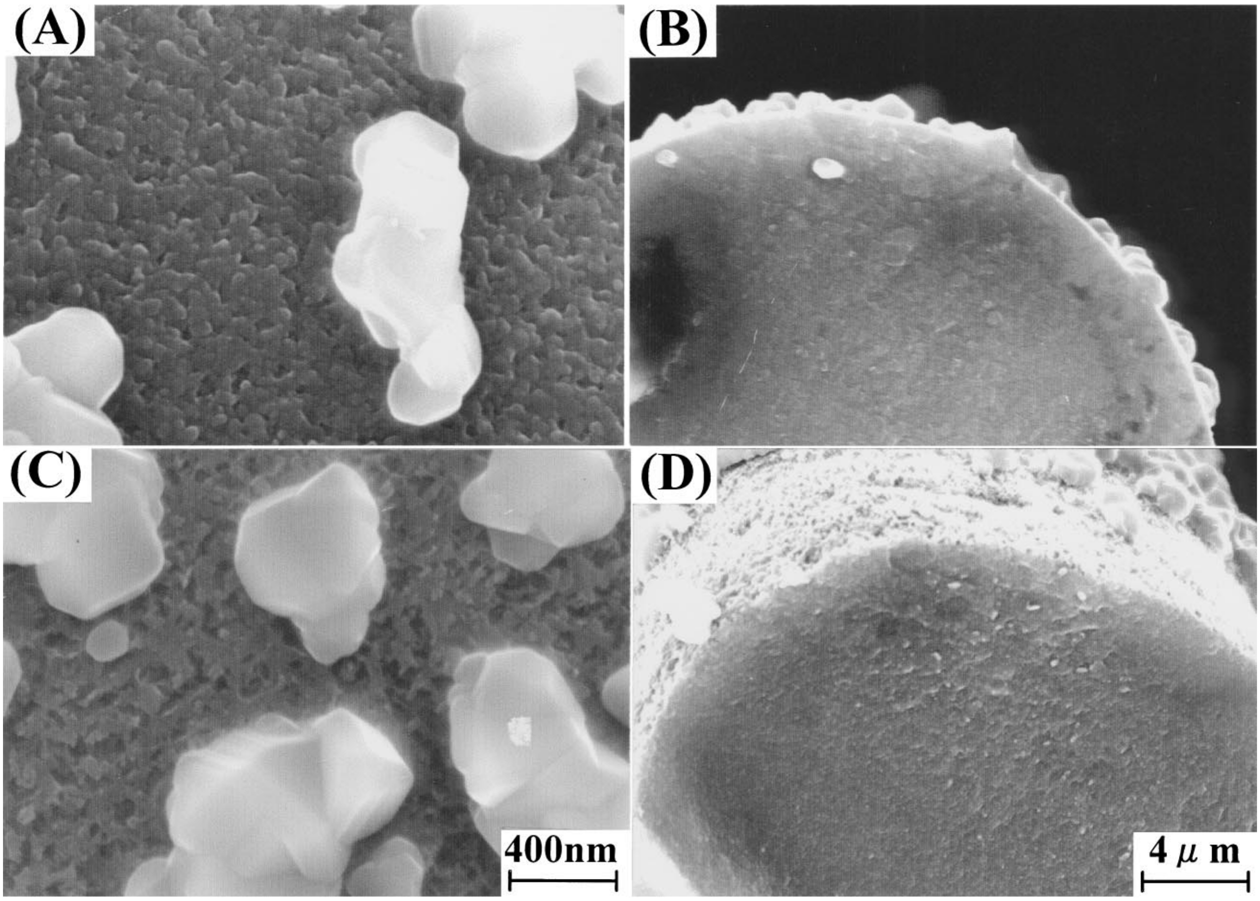

Figure 7 SEM photographs of fibers exposed to 1873 K in argon. (A), (B) Heat-treatment at 50 K/h in argon. (C), (D) Heat-treatment at 50 K/h in nitrogen.

heat-treated in argon and nitrogen coarsened considerably through the surface of fibers and within the cross-sectional area. Both fibers displayed the feature of brittle fracture, implying low levels of strength. The fiber surface was more porous for the fiber heat-treated in nitrogen than for the fiber heat-treated in argon. Vigorous gas evolution caused by the high-temperature decomposition of $SiC_XO_YN_Z$ phase is thought to produce such a porous structure. Large bulk grains were deposited on the rough surface of fibers. As discussed previously, they are β-SiC crystals produced by the gas-phase reaction [12–14].

Fig. 8 shows the morphology of the vacuum heat-treated fiber. The fiber surface had a fine-grain structure free of pore. In addition, the fracture surface also exhibited the smooth and glassy appearance in the as-heat treated state. Even after the exposure to 1873 K, the fiber surface was free from pore, though they were slightly roughened. Furthermore, the SiC crystals produced by gas-phase reaction were finely deposited on the fiber surface. This suggests that the high-temperature decomposition of SiC_XO_Y phase occurred only slightly.

3.5. Fiber strength

Fig. 9 shows the room-temperature tensile strength of silicon carbide fibers. For the fiber heat-treated in argon, there was little dependence of the strength on heating rate. The high-temperature exposure resulted in the reduction of strength from 3.5 to 1.6 GPa. When heat-treated in nitrogen, the fiber strength increased with increasing the heating rate. The fiber heat-treated at 50 K/h yielded low levels of strength: 2.6 GPa in the as-heat treated state and 1 GPa after 3.6 ks of exposure to 1873 K. On the other hand, the strength of fiber heat-treated at 600 K/h was comparable to the strength of fibers heat-treated in argon. As stated above, such results were attributable to the difference in the nitrogen solubility of fibers. The strength of the fiber heat-treated in vacuum, which was practically unaffected by the heating rate, gave high levels of value: 3.5 GPa in the as-heat treated state and 2 GPa after 3.6 ks of exposure to 1873 K.

4. Discussion

4.1. Fiber heat-treated in argon

The AES depth profile demonstrates that the oxygen-enriched layer was present on the fiber surface. Surface concentration of oxygen (about 4–8 at%) was larger than mean concentration (1.6 at%) determined by chemical analysis. Such an oxygen distribution appears to be responsible for the contamination of EB-cured PCS fiber with atmospheric gas. The oxygen in PCS-derived silicon carbide fiber exists as amorphous silicon oxycarbide, SiC_XO_Y phase [1]. At elevated temperature, the SiC_XO_Y phase decomposes into β-SiC, involving the generation of SiO and CO gases.

$$SiC_XO_Y\,(s) = SiC\,(s) + SiO\,(g) + CO\,(g) \qquad (1)$$

The high-temperature exposure caused a significant reduction of oxygen in the fiber. In addition, it caused

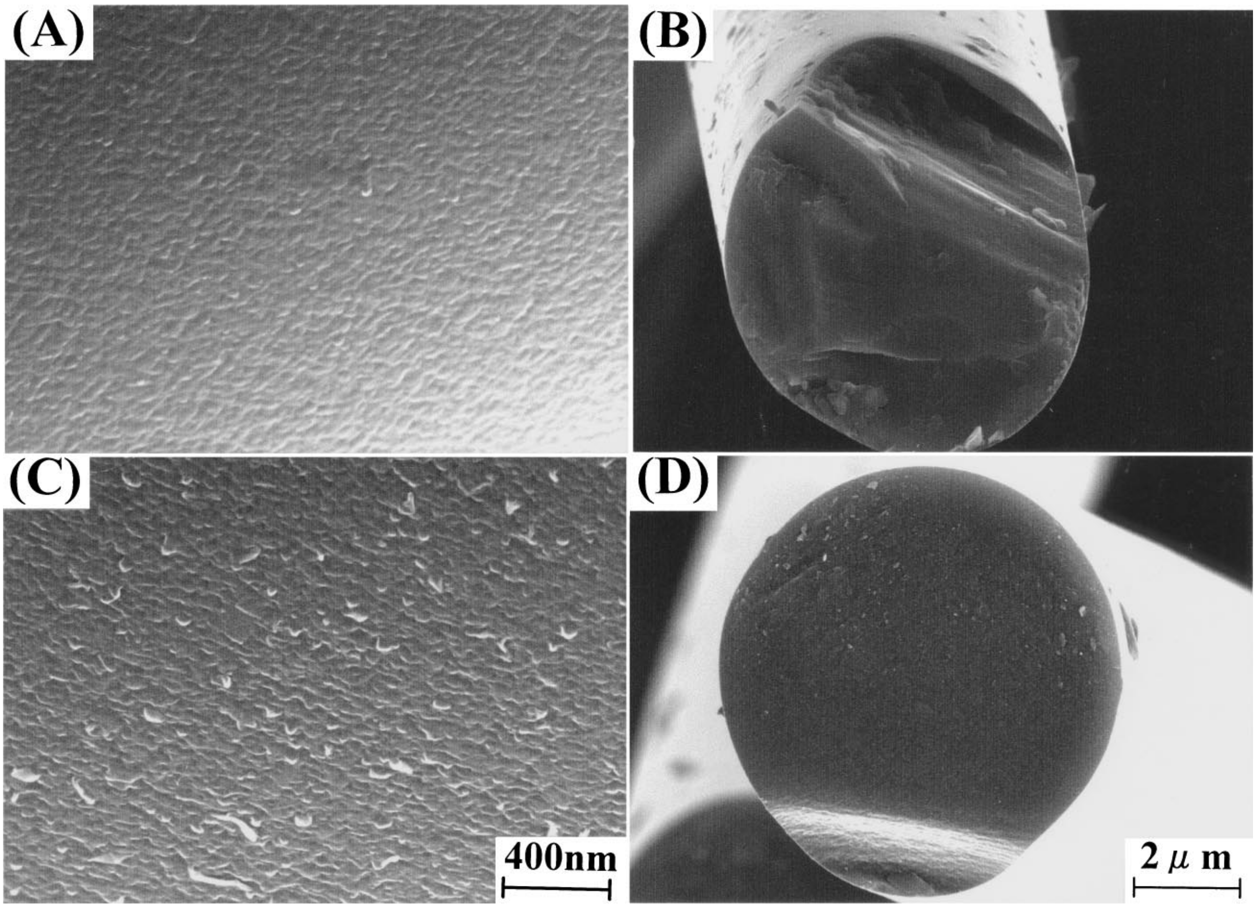

Figure 8 SEM photographs of fibers heat-treated at 50 K/h in vacuum (A, B) and of ones exposed subsequently to 1873 K in argon (C, D).

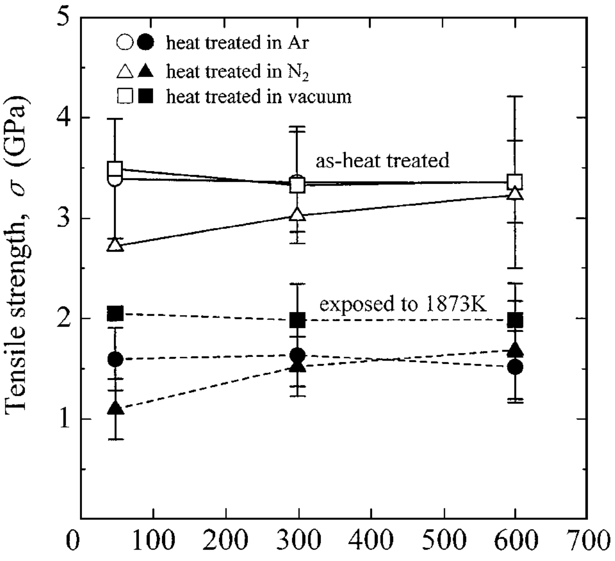

Figure 9 Tensile strength of fibers heat-treated under different atmospheres.

the inward development of the carbon-enriched layer and the increase in the C/Si mole ratio of fiber core (see Fig. 2). This result suggests that the decomposition of SiC_XO_Y phase allows to liberate mainly SiO gas. Thus, the decomposed fiber was a mixture of β-SiC and free carbon and consequently its resistivity decreased to 10^{-3} Ω m. Such a high-temperature decomposition caused the changes in the microstructure of the fiber, that is, the coarsening of β-SiC crystallites and the production of imperfections such as pores, voids and flaws (figs 6 and 7). In particular, marked change may occur in the microstructure of the fiber surface which was enriched in oxygen. Furthermore, large bulk crystals deposited on the fiber surface were the β-crystals which was produced according to the following gas-phase reaction [13]:

$$\mathrm{SiO\,(g) + CO\,(g) = SiC\,(s) + CO_2\,(g)} \qquad (2)$$

Thus, the grain coarsening and surface imperfections resulted in the degradation of fiber strength from 3.4 GPa to 1.6 GPa (Fig. 9).

4.2. Fiber heat-treated in nitrogen

The AES depth profile reveals that the surface of the fiber heat-treated in a nitrogen atmosphere was enriched in both oxygen and nitrogen (see Fig. 3). While oxygen was derived from a contamination during EB-curing treatment, nitrogen was derived from radical reactions during heat-treatment in nitrogen. According to evolved gas analysis, CH_4 and H_2 gases were evolved by the cleavage of Si-H and Si-CH_3 bonds in the range of 800 to 1000 K, resulting in the formation of the silicon-central radicals [16, 17]. Then, the carbon-central radicals were formed above 1000 K by the cleavage of C-H bonds, which involves the generation of H_2 gas. The radicals are thought to react with nitrogen gas to form the amorphous silicon oxycarbonitride ($SiC_XO_YN_Z$) phase on the fiber surface. The polycarbosilazane-derived Si-C-N fiber was principally composed of $SiC_XO_YN_Z$ phase [15]. Above 1673 K, it crystallized into the mixture of β-SiC and free carbon, involving the generation of SiO, CO and N_2 gases [15].

$$SiC_XO_YN_Z\,(s) = SiC\,(s) + C\,(s) + SiO\,(g) + CO\,(g) + N_2\,(g) \quad (3)$$

When pyrolyzed at 1723 K under a gas flow of argon, Si-C-N fiber had the decomposed layer of 150–200 nm thickness which consisted of a very high percent of carbon and only trace of oxygen and nitrogen [15]. After the 3.6 ks of exposure to 1873 K, the EB-cured PCS fiber heat-treated in nitrogen yielded the decomposed layer which was consisted mainly of carbon in the thickness of about 100 nm (see Fig. 3). The AES profiles shows that the $SiC_XO_YN_Z$ phase was nearly completely decomposed after exposure to 1873 K. Furthermore, the formation of carbon-enriched layer implies that SiO gas was principally liberated from $SiC_XO_YN_Z$ phase as well as SiC_XO_Y phase in the fiber heat-treated in argon. However, the surface concentration of oxygen and nitrogen in the fiber heat-treated in nitrogen was much higher than that of oxygen in the fiber heat-treated in argon. The fiber heat-treated in nitrogen, therefore, appears to generate more vigorously the decomposed gases than the fiber heat-treated in argon. Thus, the exposure to 1873 K produced many pores on the surface of the fiber heat-treated at 50 K/h, owing to the vigorous evolution of CO and N_2 gases (Fig. 7). Consequently, the fiber strength degraded to 1 GPa (Fig. 9). The fiber heat-treated at rapid heating rate may absorb a small quantity of nitrogen, because it is exposed to an nitrogen atmosphere over shorter period of time. Therefore, the strength of 1.6 GPa at a heating rate of 600 K/h was almost identical to that of the fiber heat-treated in argon. Finally, large change in chemical composition and microstructural change before and after high-temperature exposure allows to degrade severely the fiber strength.

4.3. Fiber heat-treated in vacuum

When SiC-C mixture is heated in vacuum at elevated temperature, gaseous silicon, Si (g), is the major volatile species [18]. On the other hand, oxygen-bearing PCS fiber may liberate SiO gas as well as gaseous silicon during heat-treatment in vacuum [4, 6, 7]. Consequently, as shown in AES depth profile (Fig. 4), the silicon-depleted layer, i.e. the carbon-enriched layer, was formed on the fiber surface even in the as-heat treated state. Fig. 10 shows the change in the pressure of reaction tube while the EB-cured PCS fiber was heated from room-temperature to 1573 K and was isothermally held in vacuum. The increase in pressure observed as three peaks at 900 and 1400 K, and during keeping at 1573 K. The analysis of gas evolved from EB-cured PCS fiber also demonstrated three peaks at 950, 1200 and 1900 K [16, 17]. From gas analysis, a drastic increase of pressure at 900 K was derived from the evolution of CH_4 and H_2, corresponding to the cleavage of Si-H and Si-CH_2 bonds [16, 17]. A weak increase in pressure at 1400 K seems to be responsible for the H_2 gas evolution caused by the cleavage of C-H bonds. Furthermore, the pressure increase observed during keeping at 1573 K is attributable to the evolution of SiO and CO gas caused by the decomposition of SiC_XO_Y phase. The formation of carbon-enriched layer suggests that SiO is main volatile species.

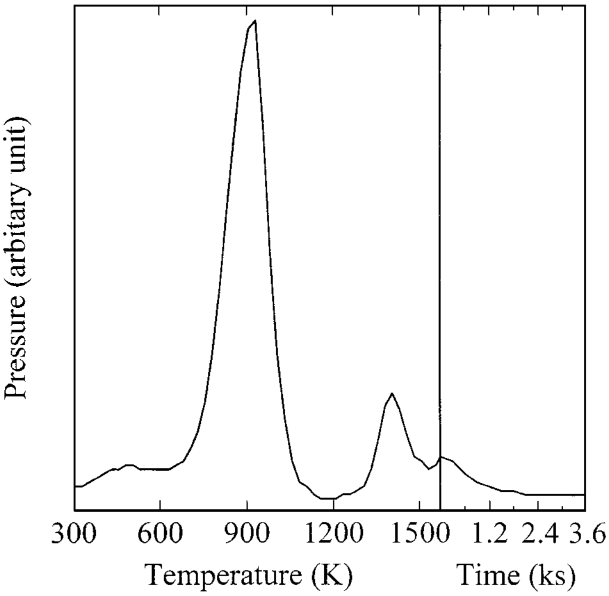

Figure 10 Change in pressure of reaction tube for fiber heat-treated at 50 K/h in vacuum.

The unstable SiC_XO_Y phase, the decomposition of which causes both the marked growth of SiC grains and the high porosity of fiber structure, was almost absent in the vacuum heat-treated fiber. Therefore, the exposure to 1873 K caused only a slight change in depth profile of fiber composition. In addition, as can be seen from Fig. 9, huge SiC grains were not formed on the surface of fiber because of the absence of reaction (2). The resistivity is a property which is highly sensitive to the change in the microstructure of silicon carbide fiber. Low resistivity is responsible for the growth of β-SiC crystallite and the formation of carbon-enriched layer. In particular, 3.6 ks of exposure to 1873 K produced the carbon rich SiC-C microstructure (the C/Si atomic ratio of 2) in which the specific resistivity and β-SiC crystallite size was 10^{-3} Ω m and 11–16 nm, respectively. There was marked coarsening of β-SiC crystallites, though there were little the changes in chemical composition and resistivity. Such a crystal coarsening is thought to take place not by decomposition of SiC_XO_Y phase but by coalescence of crystals. This seems to be because β-SiC crystallites, as a consequence of the absence of SiC_XO_Y phase, are brought into direct contact with one another. A small change in specific resitivity from 2×10^{-3} Ω m (in the as-heat treated state) to 1×10^{-3} Ω m (after exposure to 1873 K) implies that the exposure at 1873 K hardly caused the structural alternations other than the coalescence of crystals. Such results for AES and resistivity measurement suggest that surface imperfections were little formed during 3.6 ks of exposure to 1873 K. Therefore, SEM observation exhibited the smooth and pore-free appearance of the fiber (see Fig. 8) and the residual strength was in a high level of 2 GPa (see Fig. 9). On the other hand, for the fibers heat-treated in argon and nitrogen which underwent large structural alternations, the residual strength was 1.1–1.6 GPa. In spite of the absence of structural change for the fiber heat-treated in vacuum, however, the exposure to 1873 K caused the degradation of fiber strength from 3.6 to 2.0 GPa. The fiber strength is found to have a tendency to decrease with increasing the size of β-SiC crystal [12, 13]. Therefore, the above degradation of fiber strength is attributable to the coalescence of β-SiC crystals rather than the pore formation on the fiber surface.

5. Conclusions

EB-cured PCS fibers were heat-treated at 1573 K in argon, nitrogen or vacuum of 10^{-6} atm, and subsequently were exposed at 1873 K in argon.

(1) For the fiber heat-treated in argon, oxygen was retained, particularly on the surface. High-temperature exposure produced the decomposition of silicon oxycarbide phase and resulting degradation of strength.

(2) When heat-treated in nitrogen, silicon oxycarbonitride layer was formed on the fiber surface. Slow heat-treatment, as a consequence of excessive nitriding, produced a large decrease in strength. High-temperature exposure caused the decomposition of the oxycarbonitride phase and large change in surface structure, resulting in the severe degradation of strength.

(3) The vacuum heat-treatment removed nearly completely oxygen and produced a carbon-enriched layer on the fiber surface. The fiber surface was smooth and pore-free even after high-temperature exposure. The coalescence of β-SiC crystal caused a slight degradation of fiber strength.

Acknowledgement

This study was partly supported by a grant from the Ministry of Education, Science, Sports and Culture under Grant No. 11450255.

References

1. C. LAFFON, A. M. FLANK, P. LAGARDE, M. LARIDJAN, R. HAGEGE, P. OLRY, J. COTTERET, J. L. MIQUEL, H. HOMMEL and A. P. LAGRAND, *J. Mater. Sci.* **24** (1989) 1503.
2. T. MAH, N. L. HECHT, D. E. MCCULLUM, J. R. HEONIGMAN, H. M. KIM, P. KATZ and H. A. LIPSITT, *ibid.* **19** (1984) 1191.
3. K. L. LUTHRA, *J. Am. Ceram. Soc.* **69** (1986) C-231.
4. S. M. JOHNSON, R. D. BRITTAIN, R. H. LAMOREAUX and D. J. ROWCLIFF, *ibid.* **71** (1988) C-132.
5. D. J. PYSHER, K. C. GORETTA, R. S. HODDER and R. E. TRESSLER, *ibid.* **72** (1989) 284.
6. T. SHIMOO, M. SUGIMOTO and K. OKAMURA, *J. Japan Inst. Metals* **54** (1990) 802.
7. *Idem., J. Ceram. Soc. Japan (Seramikkusu Ronbunshi)* **98** (1990) 1324.
8. E. BOUILLON, F. LANGLAIS, R. PAILLER, R. NASLAIN, F. CRUEGE, P. V. HUONG, J. C. SARTHOU, A. DELPUECH, C. LAFFON, P. LAGARDE, M. MONTHIOUX and A. OBERLIN, *J. Mater. Sci.* **26** (1991) 1333.
9. C. VAHLAS, P. ROCABOIS and C. BERNARD, *ibid.* **29** (1994) 5839.
10. M. TAKEDA, Y. IMAI, H. ICHIKAWA, T. ISHIKAWA, N. KASAI, T. SEGUCHI and K. OKAMURA, *Ceram. Eng. Sci. Proc.* **12** (1991) 1007.
11. *Idem., ibid.* **13** (1992) 209.
12. T. SHIMOO, I. TSUKATA, M. NARISAWA, T. SEGUCHI and K. OKAMURA, *J. Ceram. Soc. Japan* **104** (1996) 1070.
13. T. SHIMOO, I. TSUKATA, T. SEGUCHI and K. OKAMURA, *J. Am. Ceram Soc.* **81** (1998) 2109.
14. *Idem., J. Mater. Sci.*, in press.
15. D. MOCAER, R. PAILLER, R. NASLAIN, C. RICHARD, J. P. PILLOT, J. DUNOGUES, O. DELVERDIER and M. MONTHIOUX, *ibid.* **28** (1993) 2639.
16. M. SUGIMOTO, T. SHIMOO, K. OKAMURA and T. SEGUCHI, *J. Am. Ceram. Soc.* **78** (1995) 1013.
17. *Idem., ibid.* **78** (1995) 1849.
18. G. CHOLLON, R. PAILLER, R. NASLAIN, F. LAANANI, M. MONTHIOUX and P. OLRY, *J. Mater. Sci.* **32** (1997) 327.

Received 13 September 1999
and accepted 22 February 2000